

Plasmon spectroscopy of small indium-silver clusters: monitoring the indium shell oxidation

Emmanuel Cottancin,^a Cyril Langlois,^b Jean Lermé,^a Michel Broyer,^a Marie-Ange Lebeault,^a and Michel Pellarin^{*a}

5

10 1. Oxidation of pure indium clusters: Mie calculations in a core-shell geometry

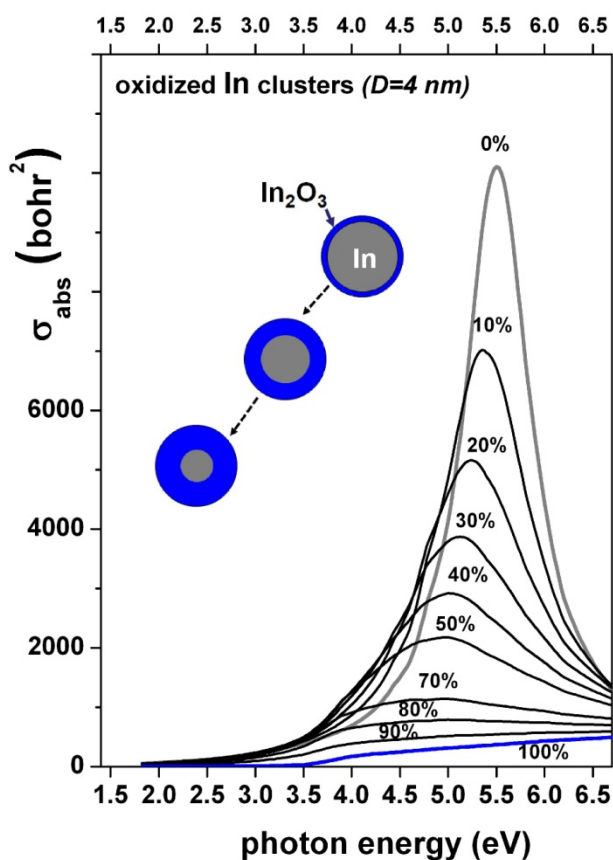


Fig.SI.1 Optical absorption cross-sections calculated in the core shell Mie theory for 4nm diameter indium clusters embedded in silica and for increasing degrees of surface oxidation. Inner surface effects on the electron collision rate in the core are included. The gray and blue curves correspond to non oxidized and fully oxidized clusters (In₂O₃), respectively

Fig.SI.1 mimicks the effect of a progressive surface oxidation of indium clusters (Mie calculations). The volume oxidation rate $\frac{V_{\text{In}_2\text{O}_3}}{(V_{\text{In}_2\text{O}_3} + V_{\text{In}})}$ varies from 0% (pure indium) to 100% (pure In₂O₃). The SPR is progressively redshifted (the

indium oxide index being larger than the silica one) and strongly damped because electron scattering by the cluster surface is all the more important that the core size is small ($\gamma_c(R_c) = \gamma_\infty + g \frac{V_F}{R_c}$). The non negligible absorbance of In₂O₃ above 3.5 eV must also be taken into account.

25

5 2. Surface plasmon resonance in disordered bimetallic InAg clusters: effective dielectric functions

In the absence of complete phase segregation, two possibilities can be considered for describing bimetallic InAg clusters: a random distribution of indium and silver nano-domains with sizes smaller than the nanoparticle diameter or an alloy disordered at the atomic scale. In the first case, an effective dielectric function for the nanoalloy $\epsilon_{\text{alloy}}^{\text{eff}(1)}$ may be defined as the volume weighted average of indium and silver permittivities:

$$\epsilon_{\text{alloy}}^{\text{eff}(1)} = x_{\text{vol}} \epsilon^{\text{In}}(\omega, R) + (1 - x_{\text{vol}}) \epsilon^{\text{Ag}}(\omega, R),$$

where $x_{\text{vol}} = \frac{1}{1 + \frac{(1-x) r_S^3(\text{Ag})}{x r_S^3(\text{In})}}$ is the volume indium concentration for an atomic concentration x ($r_S(\text{Ag})$ and $r_S(\text{In})$ are the atomic Wigner-Seitz radii of silver and indium respectively).

$\epsilon_{\text{alloy}}^{\text{eff}(1)}$ is then used to compute the absorption cross-section just as for a pure metal, keeping in mind that assigning bulk permittivities to so small domains may be questionable. In the second case, the specific dielectric function of the nanoalloy cannot reasonably be expressed in terms of a linear combination of pure element permittivities. The most suited empirical approach would then be to construct an effective dielectric function $\epsilon_{\text{alloy}}^{\text{eff}(2)}$ as the sum of a Drude-like term

$$\epsilon_{\text{alloy}}^{\text{eff},C}(\omega, R) = 1 - \frac{\langle \omega_p^2 \rangle}{\omega(\omega + i \langle \gamma(R) \rangle)}$$

involving averaged square plasmon frequencies and collision rates ($\langle \omega_p^2 \rangle = x_{\text{vol}} \omega_{\text{In}}^2 + (1 - x_{\text{vol}}) \omega_{\text{Ag}}^2$),

$$\langle \gamma(R) \rangle = x_{\text{vol}} \langle \gamma(R) \rangle_{\text{In}} + (1 - x_{\text{vol}}) \langle \gamma(R) \rangle_{\text{Ag}}$$

and a effective interband susceptibility $\chi_{\text{eff}}^{\text{IB}}(\omega)$. $\gamma(R) = \gamma_{\infty} + g \frac{v_F}{R}$ is the cluster effective electron collision rate (bulk value corrected for scattering processes at the particle surface).

In the case of pure crystalline metals, the dielectric susceptibility $\chi^{\text{IB}}(\omega)$ is related to the electronic band structure and especially to the allowed optical transitions from the deep valence band levels to empty states above the Fermi level (highest occupied level of the conduction band). They have no direct equivalent in the case of small alloyed clusters, in the absence of crystalline order at the nanoscale. Experimental or theoretical information obtained from dilute bulk alloys where the atoms of one element are inserted as impurities in the lattice of the main element is of little help in the present case of a 50%-50% stoichiometric compound. Empirical approaches then consist in defining $\chi_{\text{eff}}^{\text{IB}}(\omega)$ from the knowledge of pure element

susceptibilities $\chi_{\text{Ag}}^{\text{IB}}(\omega)$ and $\chi_{\text{In}}^{\text{IB}}(\omega)$ on the basis of effective medium theories.

Among all possible approaches, the two most common consist in:

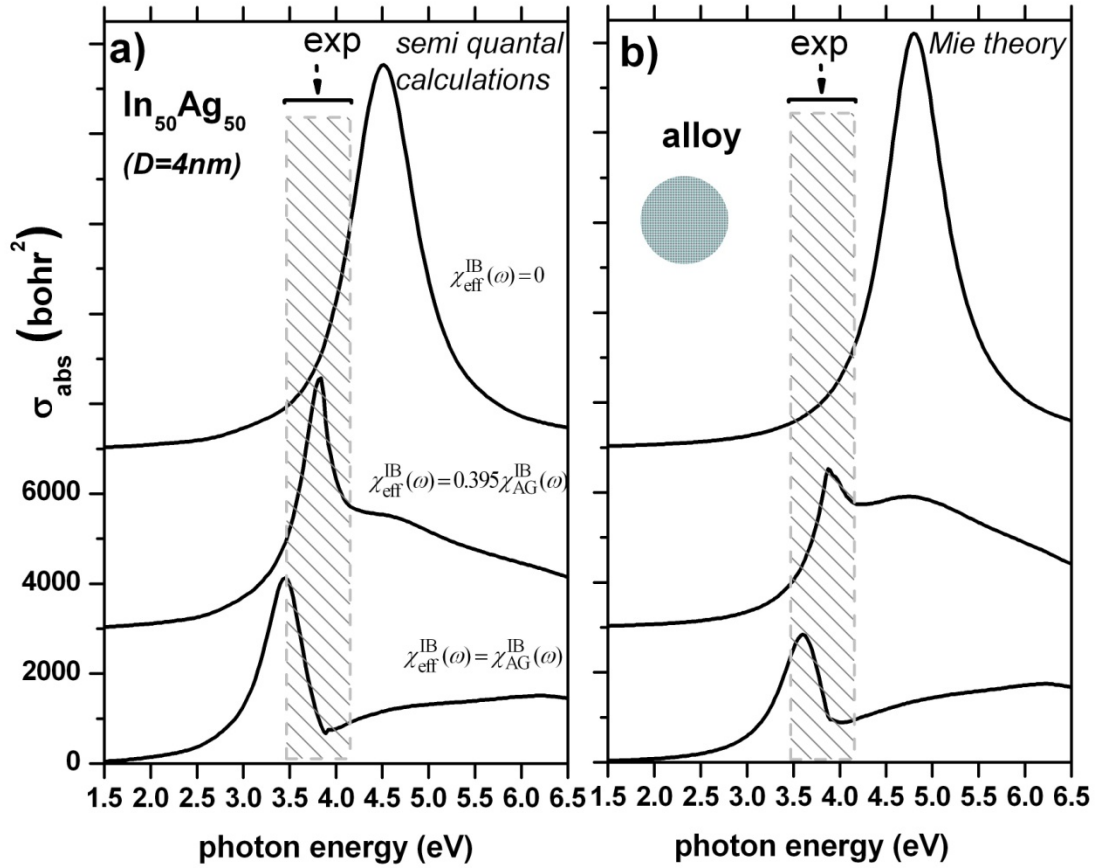
(a) expressing $\chi_{\text{eff}}^{\text{IB}}(\omega)$ as an average of both metal susceptibilities weighted by their respective volume ratio: $\chi_{\text{eff}}^{\text{IB}}(\omega) = x_{\text{vol}} \chi_{\text{In}}^{\text{IB}}(\omega) + (1 - x_{\text{vol}}) \chi_{\text{Ag}}^{\text{IB}}(\omega)$

(b) constructing an intermediate susceptibility by first defining an effective interband threshold as the weighted average of Ag and In values in the form $\omega_{\text{eff}}^{\text{IB}}(x_{\text{vol}}) = x_{\text{vol}} \omega_{\text{In}}^{\text{IB}} + (1 - x_{\text{vol}}) \omega_{\text{Ag}}^{\text{IB}}$ and making the assumption that the imaginary part of $\chi_{\text{eff}}^{\text{IB}}(\omega)$ (above $\omega_{\text{eff}}^{\text{IB}}$) can be expressed as those of pure elements in the form: $\text{Im}[\chi_{\text{eff}}^{\text{IB}}(\omega_{\text{eff}}^{\text{IB}}(x_{\text{vol}}) + \omega)] = x_{\text{vol}} \text{Im}[\chi_{\text{In}}^{\text{IB}}(\omega_{\text{In}}^{\text{IB}} + \omega)] + (1 - x_{\text{vol}}) \text{Im}[\chi_{\text{Ag}}^{\text{IB}}(\omega_{\text{Ag}}^{\text{IB}} + \omega)]$.

This amounts to establishing $\text{Im}[\chi_{\text{eff}}^{\text{IB}}(\omega)]$ from $\chi_{\text{Ag}}^{\text{IB}}(\omega)$ and $\chi_{\text{In}}^{\text{IB}}(\omega)$ by a morphing process controlled by the alloy composition (the real part of $\chi_{\text{eff}}^{\text{IB}}(\omega)$ is further obtained by a Kramers-Kronig analysis).

Details about these models can be found in Ref [1] and references therein. Hypothesis (a) gives an effective dielectric function $\epsilon_{\text{alloy}}^{\text{eff}(2)}$ (a) and hypothesis (b) gives $\epsilon_{\text{alloy}}^{\text{eff}(2)}$ (b). The optical response of nanoalloys can also be calculated within a semi-quantal approach as defined in Section 2.4 of the main text. In this case, the classical contribution of interband transitions to the dielectric screening is modeled in the same way and calculations depend on the choice made for $\chi_{\text{eff}}^{\text{IB}}(\omega)$ as in the previous (a) and (b) hypotheses. Semi-quantal calculations are comparable to classical ones using $\epsilon_{\text{alloy}}^{\text{eff}(2)}$ ((a) or (b) hypotheses) since conduction electrons provided by silver and indium atoms are not discerned.

When both metals have close electronic structures as gold and silver for instance, empirical classical descriptions using $\epsilon_{\text{alloy}}^{\text{eff}(1)}$, $\epsilon_{\text{alloy}}^{\text{eff}(2)}$ (a) or $\epsilon_{\text{alloy}}^{\text{eff}(2)}$ (b) give very similar results even if $\epsilon_{\text{alloy}}^{\text{eff}(2)}$ (b) is preferred.^{1,2} In the case of silver and indium, the situation is very different. In silver, $\omega^{\text{IB}} \cong 3.9$ eV and the hybridization between the 4d valence and the 5s4p conduction bands is important while ω^{IB} is repelled in the far UV³ for indium (the 4d band of indium is about 10 eV lower than the one



5

Fig.SI.2 (a) Semi-quantal calculations of the absorption cross-section of 4 nm diameter $\text{In}_{0.5}\text{Ag}_{0.5}$ bimetallic alloyed clusters embedded in silica for three effective dielectric function $\epsilon_{\text{alloy}}^{\text{eff}(2)}$ depending on the choice of the interband dielectric susceptibility $\chi_{\text{eff}}^{\text{IB}}(\omega)$ taken proportional to the one of silver $\chi_{\text{Ag}}^{\text{IB}}(\omega)$. The position of the experimental SPR band is indicated by the dashed area. (b) Corresponding classical Mie calculations for the same choices of $\chi_{\text{eff}}^{\text{IB}}(\omega)$ ($\epsilon_{\text{alloy}}^{\text{eff}(2)}$ type for the Drude contribution including intrinsic size effects in the electron collision rates).

10

In the present case, adopting description (b) would lead to a quasi vanishing effective susceptibility $\chi_{\text{eff}}^{\text{IB}}(\omega)$ in the visible range of interest and therefore to the absence of screening of the conduction electrons by the ionic background (for silver-rich mixed clusters, this choice is patently unphysical). This situation is mimicked in Fig. SI.2 using Mie or semi-quantal calculations (top spectra). It results in an unscreened SPR located about 5 eV. In the hypothesis (a) of an average susceptibility and because $\chi_{\text{In}}^{\text{IB}}(\omega)$ is negligible in the visible range, $\chi_{\text{eff}}^{\text{IB}}(\omega) \cong 0.395\chi_{\text{Ag}}^{\text{IB}}(\omega)$ for a 50%-50% atomic composition ($x=0.5$ and $(1-x_{\text{vol}})=0.395$). It amounts to the more acceptable hypothesis of considering that silver ions are responsible of the dielectric screening of the conduction electrons. The effective susceptibility is ruled by the polarizability of the ionic

background and could be empirically expressed as being proportional to the relative volume ratio of silver itself. This situation is illustrated in the middle spectrum of Fig.SI.2 where the SPR is now red shifted as compared to the one obtained without ionic screening (top spectra). The extreme situation of a maximum screening by assuming that $\chi_{\text{eff}}^{\text{IB}}(\omega) \cong \chi_{\text{Ag}}^{\text{IB}}(\omega)$ (interband susceptibility of bulk silver) is depicted by bottom spectra.

Fig.SI.2 is only intended to show the high sensitivity of the SPR position as regards to the modeling of the interband (dielectric) contribution entering the total dielectric function $\epsilon_{\text{alloy}}^{\text{eff}(2)}$ of the alloy. The actual effective susceptibility $\chi_{\text{eff}}^{\text{IB}}(\omega)$ certainly differs from the simple hypotheses made above. The reader can refer to exhaustive studies on diluted Ag/ In alloys for

15

30

35

25

more information^{3,4}. However, this points out the relation between dielectric screening by the polarizable ionic background and the exact position of the SPR.

Concerning the possible choice of a direct averaging of the 5 dielectric functions themselves (hypothesis $\epsilon_{\text{alloy}}^{\text{eff}(1)}$ above), the absorption spectra are qualitatively similar to those that can be

obtained from the hypothesis $\epsilon_{\text{alloy}}^{\text{eff}(2)}$ (a) with $\chi_{\text{eff}}^{\text{IB}}(\omega) = (1 - x_{\text{vol}})\chi_{\text{Ag}}^{\text{IB}}(\omega)$. This is not surprising since the same weighting procedure is used in both cases. It is applied on the total dielectric functions in the first case and on the interband part only in the second case. This is illustrated in Fig.SI.3.

15

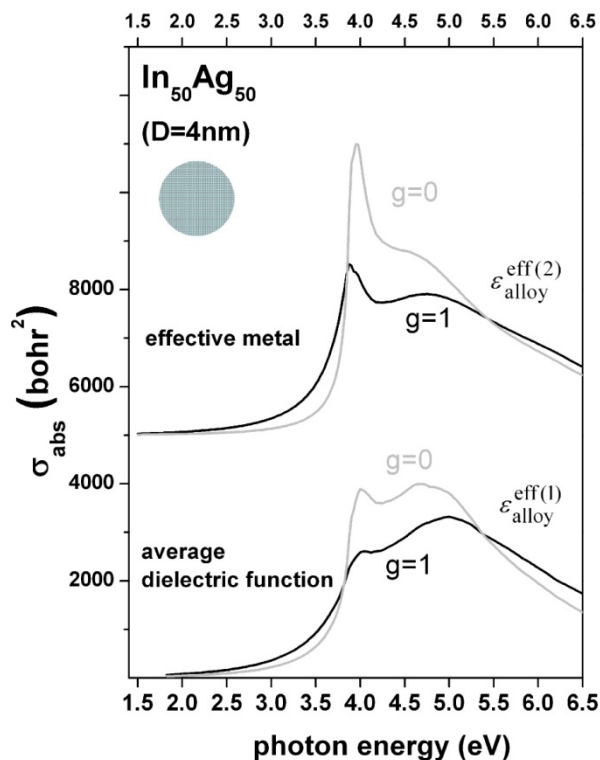


Fig.SI.3 Classical Mie calculations of the absorption cross-section of 4 nm diameter $\text{In}_{0.5}\text{Ag}_{0.5}$ bimetallic alloyed clusters embedded in silica for two different effective dielectric functions: (i) volume averaged dielectric function $\epsilon_{\text{alloy}}^{\text{eff}(1)}$ for the bottom spectra, (ii) “effective” metal dielectric function $\epsilon_{\text{alloy}}^{\text{eff}(2)}$ (a) for the top spectra. Limited free electron path effects on the collision rates are either included (black curves for $g = 1$) or neglected (gray curves for $g = 0$) (see the main text for the definition of g)

25

3. Broadening of the surface plasmon resonance in core shell In@Ag and Ag@In clusters: Mie versus semi-quantal calculations.

30

Fig.SI.4 illustrates the effect of intrinsic size effects on the width of the SPR calculated within the classical Mie theory. The

reducing of the electron mean free path through collisions with the intermediate (core-shell) interface or the cluster surface is

controlled by the choice of the g parameter in the corresponding collision rate (see main text-Section 2.2). It appears that for $g=0$

(no size effect), the SPR is much sharper and slightly blue-shifted as compared to the case $g=1$ (maximum size effect).

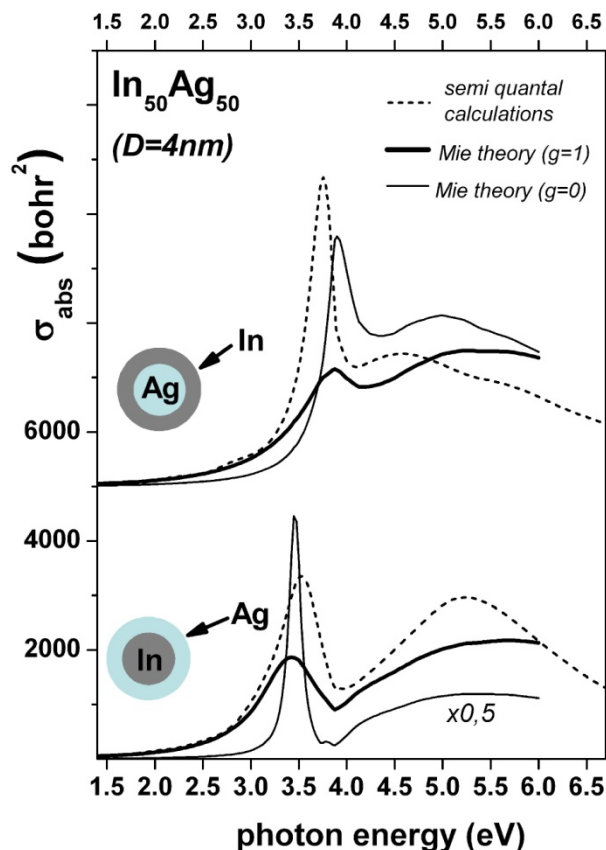


Fig.SI.4 Classical Mie calculations (full lines) and semi-quantal calculations (dotted lines) of the absorption cross section of 4 nm diameter $\text{In}_{0.5}\text{Ag}_{0.5}$ clusters in a core shell geometry and embedded in silica: $\text{Ag}@In$ (top spectra) and $\text{In}@Ag$ (bottom spectra). In Mie calculations, limited free electron path effects on the collision rates are either included (thick curves for $g=1$) or neglected (thin curves for $g=0$) (see the main text for the definition of g).

In semi-quantal calculations, the SPR broadening due to electron confinement is explicitly taken into account through the Landau damping mechanism. In Mie calculations, and apart from size effects, the resonance in the 3.5 eV-4 eV range that essentially signs the plasmonic response of silver will be all the more broadened that its coupling with indium and interband transitions is strong or in other terms that it is located in the blue region of the spectrum. This is illustrated in figure SI4 where the classical Mie spectra for $\text{Ag}@In$ (top) are more damped than for $\text{In}@Ag$ (bottom). This holds for any value of the g factor. However, the difference between spectra obtained for $g=0$ or $g=1$ (SPR width and magnitude) is much larger in the case of $\text{In}@Ag$ (bottom) since size effects on the collision rates (limited electron free path) are dominating here. The resonance is only weakly coupled to high energy processes (silver interband transition above 3.9 eV for instance). In the case of semi-quantal calculations, the correlation between width and spectral position is not as direct because the SPR is now very dependent on the magnitude of the electron spill-out which differs from one

chemical configuration to the other and that is not included in the classical formalism.

As a consequence, the proximity of semi-quantal calculations with classical ones for $g=0$ in the case of $\text{Ag}@In$ is not a proof of the absence of confinement effect as regard to the collective electron excitation. It must rather be considered as fortuitous and shows the limitations of electron collision rate modifications introduced in classical calculations of the optical response. The almost zero g value required for $\text{Ag}@In$ is actually strongly underestimated for $\text{In}@Ag$ because it would result in a SPR band much sharper in classical than in semi-quantal calculations. The better overall agreement obtained by choosing a common g value less than unity and about 0.7 (value inferred from the study of larger silver nanoparticles⁵) would not be of fundamental significance.

4. Surface plasmon resonance in core shell In@Ag clusters: effect of partial alloying.

5

Fig.SI.5 gives a comparison between SPR calculations assuming either a perfect Ag@In core shell geometry or the possible core and shell alloying with the stoichiometry of the most likely intermetallic phases observed in the bulk alloy. Spectra are similar but for the “hybrid” (partially alloyed)

structure, the resonance appears as a weaker shoulder on the low energy side of the absorption band. The dielectric function of alloyed domains is calculated according to the model $\epsilon_{\text{alloy}}^{\text{eff}(1)}$ described above.

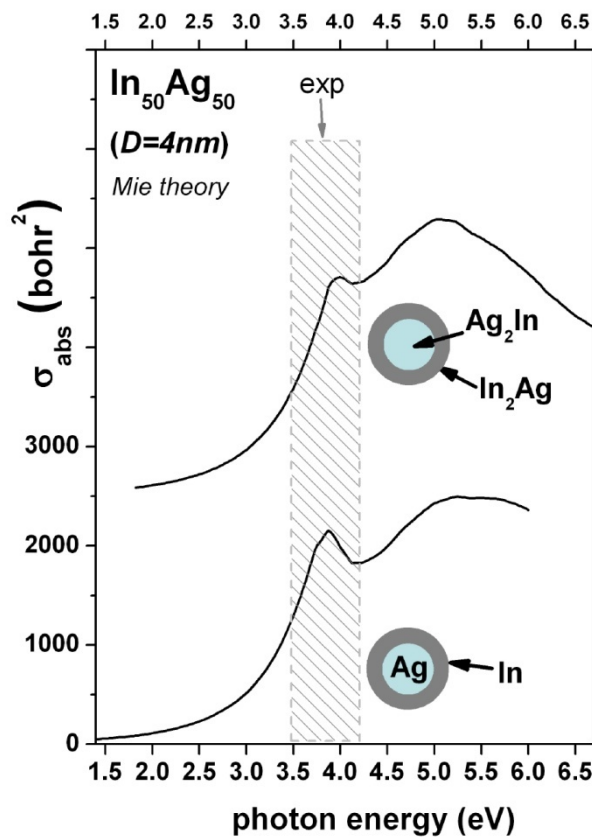


Fig.SI.5 Classical Mie calculations of the absorption cross-section of 4 nm diameter $In_{0.5}Ag_{0.5}$ clusters in a core shell geometry and embedded in silica. Bottom spectrum: pure silver core and pure indium shell. Top spectrum: Ag_2In alloyed core and In_2Ag alloyed shell. The position of the experimental SPR band is indicated by the dashed area.

25 References

^a Institut Lumière Matière, UMR5306 Université Lyon 1-CNRS, Université de Lyon, 69622 Villeurbanne Cedex, France

^b MATEIS, UMR 5510, INSA-Université Lyon 1-CNRS, INSA de Lyon, 69621 Villeurbanne Cedex, France

30 *Email :michel.pellarin@univ-lyon1.fr

1 M. Gaudry, J. Lermé, E. Cottancin, M. Pellarin, JI. Vialle, M. Broyer, B. Prével, M. Treilleux, and P. Mélinon, *Phys. Rev. B*, 2001, **64**, 085407

2 P. O. Nilsson, *Phys. Kondens. Materie*, 1970, **11**, 1

3 K. J. Kim, L. Y. Chen, and D. W. Lynch, *Physical Review B*, 1988, **38**, 13107

4 R. M. Morgan, and D. W. Lynch, *Phys Rev*, 1968, **172**, 628

5 H. Baida, P. Billaud, S. Marhaba, D. Christofilos, E. Cottancin, A. Crut, J. Lermé, P. Maioli, M. Pellarin, M. Broyer, N. Del fatti, F. Vallée, A. Sanchez-Iglesias, I. Pastoriza-Santos, and L. M. Liz-Marzan, *Nano Lett.*, 2009, **9**, 3463–3469; Jean Lermé, Hatim Baida, Christophe Bonnet, Michel Broyer, Emmanuel Cottancin, Aurélien Crut, Paolo Maioli, Natalia Del Fatti, Fabrice Vallée E, and Michel Pellarin, *The Journal of Physical Chemistry Letters*, 2010, **1**, 2922